J Fluoresc (2017) 27:1531–1540
DOI 10.1007/s10895-017-2092-4

ORIGINAL ARTICLE

NLOphoric 3,6-di(substituted quinoxalin) Carbazoles – Synthesis, Photophysical Properties and DFT Studies

Rahul D. Telore[1] · **Amol G. Jadhav**[1] · **Nagaiyan Sekar**[1]

Received: 10 January 2017 / Accepted: 4 April 2017 / Published online: 22 April 2017

Abstract Synthesis of novel 3,6-di(substituted quinoxalin) carbazole fluorophores by the condensation of 1,1′-(9-ethyl-9H-carbazole-3,6-diyl)bis(2-bromoethanone) with methyl, chloro and unsubstituted o-phenylenediamine is presented. Synthesized derivatives are well characterized by ^{1}H NMR, ^{13}C NMR, FTIR and Mass spectroscopy. Photophysical studies are carried out using solvents of varying polarities revealed positive solvatochromism and intramolecular charge transfer from carbazole (Donor) to quinoxalin (Acceptor). Intramolecular charge transfer properties are correlated by dipole moment changes and different polarity functions like Lippert–Mataga, Bilot-Kawski, Bakhshiev and Liptay plots with very good regression factors. Mulliken hush-analysis further support charge transfer characteristic. Linear and Nonlinear optical properties are explained by solvatochromic data using two-level quantum mechanical model and are correlated with computational calculations using density functional theory at B3LYP/6-31G(d) level. First hyperpolarizability value of all the synthesized compounds is found to be greater than urea by >333 times. Moreover, increase of hyperpolarizability values from non-polar to polar solvents are in good correlation with the significant charge transfer characteristic in polar solvents.

Keywords Carbazoles · ICT · NLOphoric · Solvent polarity functions · Substituted quinoxaline

Electronic supplementary material The online version of this article (doi:10.1007/s10895-017-2092-4) contains supplementary material, which is available to authorized users.

✉ Nagaiyan Sekar
n.sekar@ictmumbai.edu.in; nethi.sekar@gmail.com

[1] Department of Dyestuff Technology, Institute of Chemical Technology, Matunga, Mumbai 400 019, India

Introduction

In the designing of electro-optical materials carbazole core plays a key role acting as the donor part of D- π-A system with BODIPY [1], coumarin [2], styryl [3], quinoxaline [4] and cyanine [5] as acceptors. The carbazole moiety can be easily functionalized at 3-, 6- or 9- positions and covalently linked to other molecular moieties [6]. Substituted carbazoles are known to possess desirable photophysical properties [7, 8] as the requirement for functional applications.

The quinoxaline ring at 3 and 6 positions of carbazole acts as an acceptor through covalent bond or π bridge which leads to D-π-A system with fluorescent properties [9]. The molecules having D- π-A bridge are good candidates for electronics as well as biological applications such as dye sensitizer solar cell (DSSC) with light harvesting properties [10], organic light emitting diode OLED [11], lasers [12], optoelectronics [13], semiconductors [14], sensors [15–18] and bio-imaging [19, 20]. Electron accepting quinoxaline moieties have been exploited for the construction of electron transporting materials suitable for OLED fabrication [21–23]. Exceptionally, carbazole and oxadiazoles, quinoxaline or dicyanovinyl conjugates have been demonstrated to function as dual transport materials with promising emission characteristics [24, 25]. Such small arrangement of molecules, respond to photoexcitation with an intramolecular charge transfer from the donor to the acceptor moiety through π-conjugation [26].

A simple experimental method used to determine optical second order polarizability of the molecules on the basis of second harmonic generation (SHG) was developed by using a two-level quantum mechanical model [27–30]. We have selected this method which is based on solvatochromism, and solvent dependence of the UV-visible absorption and emission spectrum of the synthesized quinoxaline derivatives [28, 31, 32]. The solvatochromic method for determination of first

order hyperpolarizability β_{ijk} or β_{xxx} (β_{CT}) was successfully applied first by Paley et al. [27].

The geometry of synthesized compound was optimized with density functional theory (DFT) [33]. The time dependent density functional theory (TD-DFT) computation has been utilized to predict photophysical properties and polarizability values [34]. The DFT and solvatochromism based on conventional correlation between the NLO properties and their parameters like the linear polarizability (α), and first (β_0) and second (γ) hyperpolarizabilities of π-conjugated system.

In this paper we are reporting synthesis of 9-ethyl-3,6-di(quinoxalin-2-yl)-9H–carbazole derivatives with orderly change in substituents on quinoxaline ring. The geometry of all the carbazole based quinoxalines were optimized with DFT using B3LYP method and 6-31G(d) basis set. TD-DFT computation has been utilized to predict photophysical properties and nonlinear optical properties of the synthesized quinoxaline and the theoretical values are correlated with experimental values.

Experimental Section

Materials and Equipment

All the reagents and solvents were purchased from the S. D. Fine Chemicals Pvt. Ltd. and used without purification. All the solvents used were of spectroscopic grade. Melting points were recorded by open capillary on Sunder Industrial Product and are uncorrected. UV-Visible absorption measurements were carried out using a Perkin Elmer spectrophotometer with 1 cm quartz cells. The excitation wavelengths were taken as the absorption maxima (λ_{max}) of the compounds. The scan range was 250 to 650 nm. Fluorescence emission spectra were recorded on Cary Eclipse fluorescence spectrophotometer (Varian, Australia) using 1 cm quartz cells. ^{1}H NMR spectra were recorded on VNMR 500-MHz instrument using TMS as an internal standard in $CDCl_3$ and DMSO as a solvent.

Computational Methods

The ground state (S_o) geometry of the **6a**-**6c** in their C_1 symmetry were optimized using the tight criteria in vacuum as well as in different solvents using DFT [35]. The vibrational frequencies at the optimized structures were computed using the B3LYP/6-31G(d) method to verify that the optimized structures correspond to local minima on the energy surface [36–38]. The vertical excitation energies at the ground-state equilibrium geometries were calculated with TD-DFT. All the computations were carried out in vacuum phase and also in solvent of different polarities using the Polarizable Continuum Model (PCM) [39, 40]. All the electronic structure computations were carried out using the Gaussian 09 program [33].

Relative Quantum Yield Calculations

Quantum yields (**ϕ**) of compounds **6a**–**6c** in various solvents were evaluated. Relative quantum yields were measured using quinine sulfate in 0.1 N H2SO4 as standard (**ϕ** = 0.546). Quantum yields were calculated using the comparative method [41, 42]. Absorption and emission characteristics of the standard (in 0.1 N H2SO4) and the compounds in various solvents were measured at different concentrations (1, 2, 3, 4, and 5 μM). Emission intensity values were plotted against absorbance values and linear plots were obtained. Gradients were calculated for the standard and the compounds in each solvent keeping slit width constant at 5. Relative quantum yields of the synthesized compounds in various solvents were calculated by using the Eq. 1 [41, 42].

$$\phi_x = \phi_{st} X \frac{\mathrm{Grad}_x}{\mathrm{Grad}_{st}} X \frac{\eta_x}{\eta_{st}} \quad (1)$$

where,

ϕ_x	Quantum yield of compound
ϕ_{st}	Quantum yield of standard sample
Grad_x	Gradient of compound
Grad_{st}	Gradient of standard sample
η_x	Refractive index of solvent used for Compound
η_{st}	Refractive index of solvent used for standard sample

Quantum yields of all the dyes in various solvents are tabulated in Tables 1, **S1** and **S2.**

Experimental

*Preparation of 9-ethyl-9H-carbazole **2***

The compounds 5 and 7 were prepared by the reported method [12].

*Preparation of 1,1′-(9-ethyl-9H-carbazole-3,6-diyl) bis(2-bromoethanone) **4***

The compounds 4 were prepared by the reported method [43].

*General Procedure for Synthesis of Carbazole Substituted Quinoxaline **6a-6c***

A mixture of 1,1′-(9-ethyl-9H-carbazole-3,6-diyl)bis(2-bromoethanone) **4** (0.5 g, 0.0014 mol), substituted ortho-phenylenediamine **5a** (0.308 g, 0.0028 mol) and potassium carbonate (0.579 g, 0.0042 mol) in DMF (15 ml) was stirred at 90 °C for 3–4 h. After completion of the reaction, the mass was poured into the 50 mL ice cold water. The resulting solids ***6a-6c*** were filtered; washed with water and purified by column chromatography on 100–200 mesh silica with

Table 1 Effect of solvent polarity on photophysical properties of **6a**

6a	λ_{abs} (nm)		ε ($Lmol^{-1}$ cm^{-1})	λ_{emi} (nm)		Stokes shift (cm^{-1})	ϕ	*f (Oscil. Strngth.)*	
	Experimental	Computed		Experimental	Computed			Experimental	Computed
Toluene	389	405.81	24,400	432	434.8	2558.7	0.120	0.348	0.785
Dioxane	387	404.7	10,000	468	432.59	4472.2	0.020	0.289	0.766
DCM	386	411.21	18,800	468	441.4	4539.2	0.059	0.111	0.750
$CHCl_3$	387	409.23	28,000	452	438.41	3715.8	0.055	0.267	0.761
EtOAc	389	409.51	22,000	442	439.16	3082.5	0.018	0.404	0.737
Acetone	384	412.09	9600	470	442.43	4765.0	0.074	0.108	0.728
ACN	362	412.46	36,800	490	442.85	7216.1	0.025	0.430	0.722
DMF	390	413.3	22,800	480	444.08	4807.6	0.026	0.338	0.748
DMSO	394	413.32	19,600	498	444.08	5300.3	0.033	0.310	0.744

ε: Molar extinction coefficient, ϕ: Quantum yiled, *f: Oscillator strength*

chloroform/methanol as eluent. The synthesized compounds are well characterized by FT-IR, ^{1}H NMR, ^{13}C NMR and Mass (**Supporting Information**).

1. 9-Ethyl-3,6-di(quinoxalin-2-yl)-9H-carbazole **6a**

Color: Yellow solid, Yield: 72%, M.P.: 222-224 °C.
FT-IR (cm^{-1}): 1593 (-C = N-), 1541 (-C = C-), 1486 (-Ar).
^{1}H NMR (500 MHz, DMSO-d_6): 1.41 (t, 3H), 4.60 (q, 2H), 7.81 (td, 2H), 7.88 (m, 4H), 8.12 (d, 2H, J = 7.1 Hz), 8.17 (d, 2H, J = 7.3 Hz), 8.56 (d, 2H, J = 6.9 Hz), 9.40 (s, 2H), 9.79 (s, 2H).
^{13}C NMR (125 MHz, DMSO-d_6): 14.37, 38.00, 110.81, 120.90, 123.62, 126.26, 128.05, 129.34, 131.00, 141.86, 142.10, 144.41, 152.18.
Mass: 455 (M + 1).

2. *9-Ethyl-3-(6-methylquinoxalin-2-yl)-6-(7-methylquinoxalin-2-yl)-9H carbazole* ***6b***:

Color: Yellow solid. Yield: 56%.
M.P.: 202-204 °C.
FT-IR (cm^{-1}): 1600 (-C = N-), 1540 (-C = C-), 1487 (-Ar).
^{1}H NMR (500 MHz, $CDCl_3$): 1.51 (t, 3H), 2.62 (s, 6H), 4.44 (q, 2H), 7.56 (m, 4H), 7.96 (s, 1H), 8.00 (d, 2H, J = 8.6 Hz), 8.07 (d, 1H, J = 8.3 Hz), 8.38 (d, 2H, J = 7.9 Hz), 9.05 (s, 2H), 9.42 (s, 2H).
^{13}C NMR (125 MHz, $CDCl_3$): 13.91, 21.87, 38.08, 109.37, 120.26, 125.66, 127.99, 128.52, 131.23, 132.45, 139.41, 139.72, 140.65, 140.89, 141.27, 141.64, 141.70, 142.51, 142.59, 143.39, 151.57, 152.24.
Mass: 480 (M + 1).

3. *3-(6-Chloroquinoxalin-2-yl)-6-(7-chloroquinoxalin-2-yl)-9-ethyl-9H-carbazole* ***6c****:*

Color: Greenish yellow solid, Yield: 52%, M.P.: 218–220 °C.
FT-IR: 1598 (-C = N-), 1539 (-C = C-), 1483 (-Ar), 829 (-C-Cl).
^{1}H NMR (500 MHz, $CDCl_3$): 1.56 (t, 3H), 4.51 (q, 2H), 7.63 (d, 2H, J = 8.5 Hz), 7.68 (d, 1H, J = 7.1 Hz), 7.71 (d, 1H, J = 6.8 Hz), 8.14 (d, 2H J = 2 Hz), 8.16 (d, 2H, J = 9.4 Hz), 8.42 (t, 2H), 9.10 (s. 2H), 9.51 (d, 2H, J = 6.6 Hz).
^{13}C NMR (125 MHz, $CDCl_3$): 13.94, 38.17, 109.60, 120.47, 123.95, 125.95, 126.048, 128.02, 128.21, 130.02, 130.25, 130.49, 131.36, 136.16, 139.60, 142.08, 142.75, 143.42, 144.20, 152.93.
Mass: 521 (M + 1).

Results and Discussions

Synthesis

Compounds **6a-6c** were synthesized by using carbazole (**1**) as starting material (Scheme 1). The first step involved N-substitution of carbazole **1** by the diethylsulphate resulted into intermediate **2**. Friedel-Crafts reaction was carried out on intermediate **2** at the 3- and 6- positions by using bromoacetyl bromide to give intermediate **4**. This intermediate **4** was treated with different substituted ortho-phenylenediamine derivatives in presence of potassium carbonate in DMF at room temperature to yield **6a-6c**. All the synthesized compounds were purified by column chromatography on silica with chloroform/methanol as eluent.

Absorption and Emission Spectra in Different Solutions

Absorption and emission spectra of compounds **6a-6c** were recorded in varying polarity solvents **(Figs. S1-S3)** and the relevant parameters were compiled in Tables 1, **S1** and **S2**. Compounds **6a-6c** showed a broad and relatively intense absorption band around 390–410 nm attributable to the

Scheme 1 Synthesis of carbazole based quinoxaline derivatives

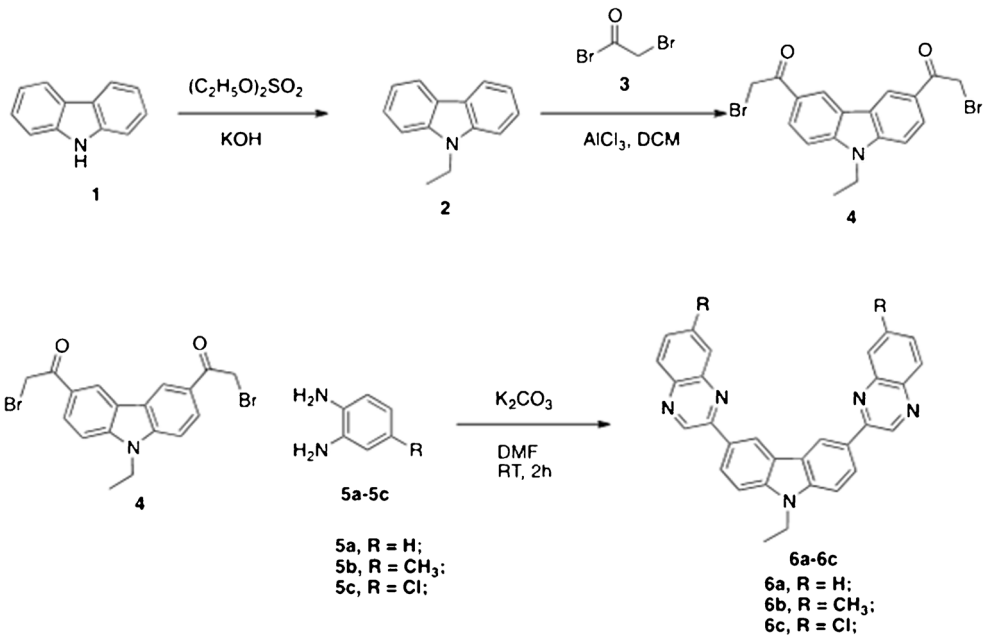

electronic transition originating from the π-molecular orbitals. But in acetonitrile they showed hypsochromic shift of lower degree around the 360–370 nm. The red-shifted absorption was observed for the arylamine derivatives (**6b** and **6c**) with expressive involvement of conjugative delocalization in the ring from donor (carbazole) to acceptor (quinoxaline) [44]. Different substitution at 6th position of aryl ring of the arylamine showed effect on absorption maxima. Hydrogen atom substitution showed hypsochromic shift as compared to chloro and methyl substitution on 6th positions. This may be due to good +I (inductive effect) of methyl group [45] and +M (mesomeric effect) of chloro group [46] as compared to hydrogen. The introduction of methyl and chloro groups as electron-donating substituents increases the electron density of quinoxaline ring. On comparing dyes **6b** and **6c** there may be reduction of accepting ability of quinoxaline core, which cause blue shift in absorption for methyl (**6b**) as compared to chloro-substituted quinoxalines (**6c**).

All the dyes studied in this work exhibited a slight red shift in emission maxima from non-polar to polar solvents. This result indicates that compounds exhibited positive solvatochromism, leading to gradual increase in the Stokes shift on increasing the solvent polarity. This mainly originates from the difference in the dipole moments of the molecule in the ground state and the excited states, interactions such as dipole-dipole, hydrogen bonding and solvation. The dipole moment ratios from ground state to excited state μ_e/μ_g are calculated and tabulated **(Table S3)**. The red-shifted emission observed for the arylamine derivatives (**6b** and **6c**) expressed the involvement of conjugative delocalization in the ring. The effects of solvent polarity on the emission are shown in **Figs. S1-S3** for the compounds **6a-6c**.

The compounds **6a-6c** exhibited broad emission bands with maxima at **6a** 498 nm, **6b** 488 nm and **6c** 514 nm in DMSO, which can be indicative of the intramolecular charge-transfer (ICT) transition due to the dipolar interaction. All the compounds showed moderate quantum efficiencies in nonpolar solvents but in case of polar solvents, the quantum yield decreased which may due to the dipolar interaction between molecule and solvents.

Dipole Moment Changes of the **6a-6c** *on Photoexcitation*

The ICT feature of the compounds **6a-6c** can be evaluated by Lippert–Mataga plots [Eq. (1)] [38–40]. The positive solvatochromism indicates that excited states of molecules are more stable in polar solvents. This can happen due to the ICT. These common solvent effects on the molecules were described solvatochromism properties by Lippert-Mataga Eq. 2. Lippert-Mataga equation (Eq. 2) was used to estimate change in dipole moment on photoexcitation as a function of the solvent polarity.

$$\Delta\nu = \frac{2\Delta f}{4\pi\varepsilon_0\hbar c a^3}\left(\mu_{e-}\mu_g\right)^2 + b$$
$$\Delta f = \frac{\varepsilon-1}{2\varepsilon+1} - \frac{n^2-1}{2n^2+1} \quad (2)$$

where,

$\Delta\nu$	ν_{abs} - ν_{em} stands for Stokes shift,
ν_{abs} and ν_{em}	are absorption and emission (cm^{-1}),
$\hbar$	Planck's constant,
c	velocity of light in vacuum,
a	Onsager cavity radius,

b	constant,
Δf	orientation polarizability,
μ_g	ground-state dipole in the ground-state geometry,
μ_e	excited-state dipole in the excited-state geometry,
ε_0	permittivity of the vacuum,
$(\mu_e\text{-}\mu_g)^2$	proportional to the slope of the Lippert-Mataga plot.

The Lippert-Mataga plots of the Stokes shift of compounds **6a-6c** against orientation polarizability showed very good regression (**Fig. S4**).

The polarity plots of the compounds **6a-6c** show good regression factors with good charge transfer. In **6a** regression factor was 0.74 and in **6b** was 0.77 with good charge transfer. In **6c** very good regression was observed (about 0.81 with good linearity). The dipole moment changes in compounds **6a-6c** inferred that the ICT features in the molecules are significant. The compounds **6a-6c** have μ_e/μ_g ratio calculated by various method like Bilot-Kawski, Bakhshiev and Liptay. The fact that the values are less than unity implies that the excited state is less polar (**Table S3**). These results are due to the electron withdrawing quinoxaline moiety on carbazole ring at 3rd and 6th position, which induce ICT.

Oscillator Strength and Transition Dipole Moment

Oscillator strength is dimensionless quantity that expresses the probability of absorption and emission properties in energy levels, which helps to understand charge transfer within the molecules. It was simply described by number of electron transition from ground to excited state. Oscillator strength (f) can be calculated using the following Eq. 3 [41].

$$f = 4.32 \times 10^{-9} \int \varepsilon(\nu) d\nu \tag{3}$$

where ε is the extinction coefficient (L mol^{-1} cm^{-1}), and ν represents the wavenumber (cm^{-1}). From this equation we have calculated oscillator strength for the synthesized carbazole based quinoxaline derivatives **6a-6c** and tabulated in **Table S4**.

By using the value of f, we have calculated transition dipole moment, which was the difference in electric charge distribution between a ground and excited state of the molecule. The transition dipole moment for absorption (μ_a) was the measurement of the probability of radiative transitions which have been calculated in Debye unit in different solvent environments using the Eq. 4 [47]. The transition dipole moment was increased with increase in the oscillator strength for all compounds **6a-6c**

$$\mu_a^2 = \frac{f}{4.72 \times 10^{-7} \times \nu} \tag{4}$$

where,

μ_a	is transition dipole moment (D),
f	is oscillator strength,
ν	is wavenumber (cm^{-1}).

The carbazole-based quinoxaline derivatives **6a-6c** have good transition dipole moment. Observed results show that the carbazole and quinoxaline moieties have good charge transfer within the small system. We obtained transition dipole moment up to 6 D for **6a-6c** molecules from the relationship between the Stokes shifts (cm^{-1}) and the solvation parameter tabulated in **Table S4**.

DFT Calculations

To investigate the structure-electronic property relationship in the carbazole based quinoxaline, we have performed DFT calculations in Gaussian. We optimized the molecular structure of compounds **6a-6c** in maximum solvent using B3LYP method and 6-31 g(d) as basic set. The lowest energy transitions resulting from the theoretical study along with their energy, oscillator strengths, absorption emission maxima, and the compositions in terms of molecular orbital contributions.

Optimized Geometries of 6a-6c

Ground state geometries of the carbazole based quinoxaline derivatives were optimized at B3LYP/6-31G(d) basic set. A small twisting was observed between C15-C14-C44-C58 (**6a**: 20.3, **6b**: 20.18 and **6c**: 18.25) (Fig. 1**)** in toluene. From the optimized geometries, it is clear that the slight twisting of the donor carbazole moiety from the quinoxaline ring by an angle 20^o in all the derivatives. The distribution of HOMO and LUMO are well separated within the molecule 6a-6c and a significant overlap is present.

Electronic Vertical Excitation Spectra (TD-DFT)

The absorption band at lower energy with higher oscillator strength is due to ICT and is characteristic of donor-π-acceptor molecules. These ICT bands for all the dyes mainly occurred due to the electronic transition from HOMO to LUMO. The compound **6a** shows blue shifted absorption in acetonitrile (362 nm) and red shifted absorption in DMSO (394 nm). The vertical excitation of 6a was computed and it shows blue shift absorption in dioxane (404 nm) and slightly red shift in DMSO (413 nm). Similar solvatochromic results were obtained for compounds 6b and 6c. The trend observed in vertical excitations of carbazole based quinoxaline

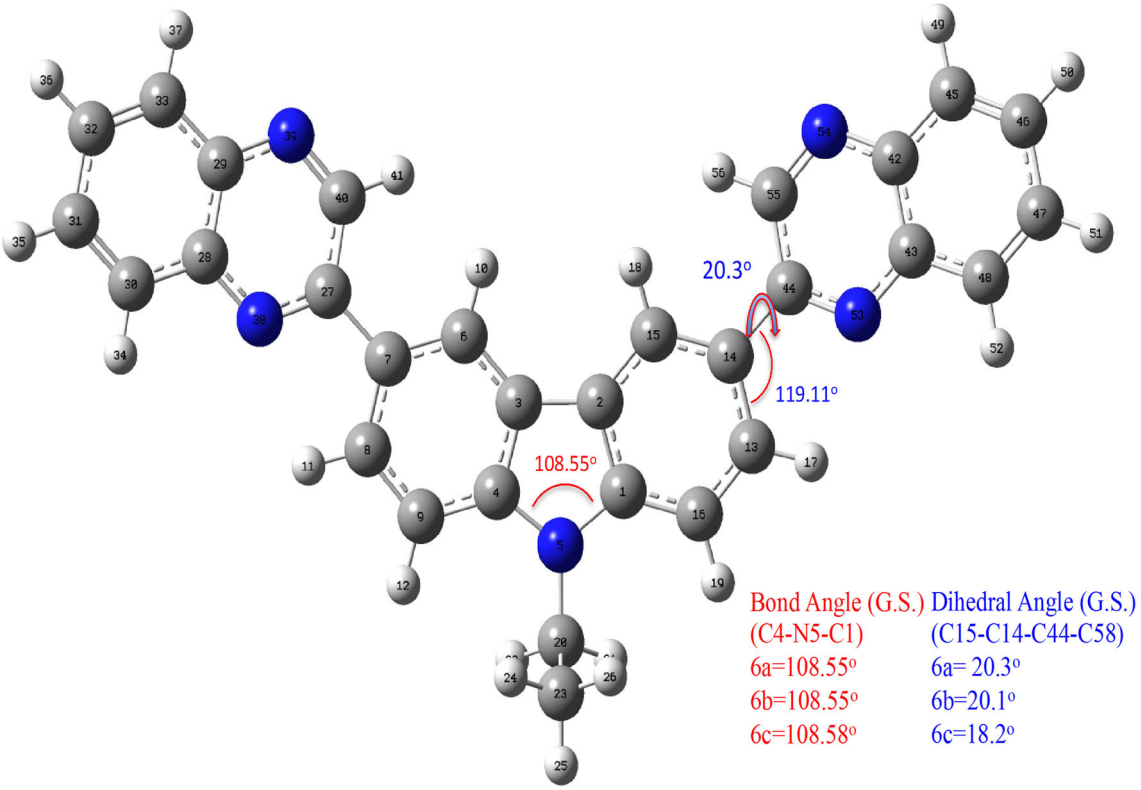

Fig. 1 Dihedral angles and bond angles in **6a-6c**

compounds were very similar to the absorption spectra (Table 1 **and S1, S2**).

Frontier Molecular Orbitals

The frontier molecular orbitals were studied to understand the electronic transition and charge delocalization within these π-conjugated systems The energy band gap in **6a** 2.29 eV, 6b 2.31 eV and **6c** 2.15 eV in toluene.

The electronic distributions in the HOMO and LUMO for the all compounds (**6a-6c**) are presented in the (**Fig. S5-S7**) with oscillator strength and band gap (eV) in toluene. The HOMO diagram of **6a** and **6b** shows that the electron density is delocalized over the carbazole ring, with maximum components arising from the carbazole nitrogen from the π conjugation to the end of quinoxaline ring. In the LUMO, maximum electron density localized on quinoxaline ring (**Fig. S5-S7**). In case of **6c**, HOMO has maximum electron density localized at chlorine on the quinoxaline ring. The LUMO showed maximum electron density located on the quinoxaline ring and carbazole ring is totally unaffected by electron delocalization (**Fig. S7**). The observations indicate that quinoxaline core enhances the electron-accepting ability and drifts the electron-density toward it and the effect is highly dependent on the powerful donor like carbazole ring. Stronger donor such as carbazole pushes more electron density towards the quinoxaline core. The trend observed for the absorption maxima of the carbazole based quinoxaline derivative in all the solvent is well supported by the vertical excitation theoretical computations and results are good agreement with the experimental absorption.

Nonlinear Optical (NLO) Properties by Solvatochromic and DFT Method

The nature and the length of π-conjugated system for NLO properties were investigated by using DFT method. Optimized geometries at B3LYP/6-31G(d) levels were used for evaluation of NLO properties of all dyes. Due to an effective ICT, the quinoxaline derivatives must show significant NLO properties. The strong ICT containing quinoxaline derivative and their first and second order NLO properties were studied.

Molecular Nonlinearity

Organic molecule with small π-conjugated system is well known for NLO property. These systems have strong π-configuration with ICT characteristics and commonly provide good arrangement for electrons to excite from ground to excited state on photo-excitation. NLO properties do not depend only on the nature of the strong conjugation, but also on the substituent positions and the geometry of the molecule. Carbazole linked to quinoxaline possess rotating single bonds in the π-conjugation resulted into change in the dihedral angles, which enhance the polarizability of these molecules.

Linear Optical Properties by Solvatochromism

Calculation of α_{CT} and μ_{CT} from the Solvatochromic Data

The linear polarizability α_{CT} was evaluated experimentally for the the dyes **6a**-**6c**. The values are obtained by two-level model using UV-vis absorption/emission spectroscopy. The solvatochromic method can also be utilized in determination of the dipole moment of the lowest lying charge transfer excited state. α_{CT} are calculated by using the Eqs. 5 and 6. And all α_{CT} values are calculated for quinoxaline derivatives (**6a**-**6c**), and are tabulated in (Table 2 **S5, S6)**.

$$\alpha_{CT} = \alpha_{xx} = 2\frac{\mu_{eg}^2}{E_{eg}} = \frac{2\mu_{eg}^2\lambda_{eg}}{hc} \tag{5}$$

where,

x	direction of charge transfer,
h	Planks constant,
c	velocity of light in vacuum,
λ_{eg}	The wavelength of transition from the ground state to excited state,
μ_{eg}^2	The transition dipole moment, that is related to the oscillator strength f.

$$\mu_{eg}^2 = \frac{3e^2h}{8\pi^2mc} \times \frac{f}{\overline{\nu}_{eg}} \tag{6}$$

where,

m	mass of electron,
f	oscillator strength,
$\overline{\nu}_{eg}$	Absorption frequency,
e	charge on electron,

The oscillator strength can be obtained by integrated absorption coefficient.

Calculation of β_0 from the Solvatochromic Data

The two level model used to determine solvent dependent hyperpolarizability is based on the Oudar equation.

$$\beta_{CT} = \beta_{xxx} = \frac{3}{2h^2C^2} \times \frac{\overline{\nu}_{eg}^2\mu_{eg}^2\Delta\mu_{CT}}{\left(\nu_{eg}^2-\nu_L^2\right)\left(\nu_{eg}^2-4\overline{\nu}_L^2\right)} \tag{7}$$

where,

x	direction of charge transfer,
h	Planck's constant,
c	speed of light in vacuum,
μ	transition dipole moment,
ν_{eg}	transition frequency,
ν_L	frequency of the reference incident radiation to which the β value would be referred,
$\Delta\mu_{CT}$	difference between the charge transfers excited state and ground state dipole moment.

The static β_{CT} is obtained from the above Eq. 7 as under the static conditions the value of ν_L = 0. The values for first hyperpolarizability obtained using the solvatochromic method (Table 2**, S5, S6**) is based on several assumptions, and thus allow only approximate estimate of dominant tensor of total hyperpolarizability along the direction of charge transfer, which is the major contributor to the total hyperpolarizability. Though the values are approximate it has advantages over the other well-known expensive method.

Calculation of solvatochromic descriptor of $\langle\gamma\rangle_{SD}$ from the solvatochromic data

The third order hyperpolarizability $\langle\gamma\rangle_{SD}$ at molecular level originating from the electronic polarization in the non-resonant region can be treated by a three-level model

Table 2 Measured linear optical properties and static first hyperpolarizability of **6a** in different solvent

6a	α (10^{-8}) (cm) [a]	λ_{max} (nm) [b]	ν_{max} (cm^{-1}) [c]	$\Delta\mu_{CT}$ (10^{-17}) (esu) [d]	μ^2_{eg} (10^{-35}) ($esu\ cm)^2$ [e]	β_{CT} (10^{-30}) (esu) [f]	γ (10^{-35}) (esu) [g]
Toluene	5.91	389	25,706	2.24931	2.04701	26.4493	7.44752
1,4-Dioxane	5.95	387	25,839	2.27218	1.88198	24.3123	6.9085
DCM	5.99	386	25,906	2.29513	2.73478	35.5018	1.0000
$CHCl_3$	6.11	387	25,839	2.36445	1.93689	26.0377	7.713
EtOAc	6.19	389	25,706	2.41104	1.3628	18.8747	5.7978
Acetone	6.02	384	26,041	2.3124	2.02072	26.1563	7.4950
ACN	6.07	362	27,624	2.34127	2.16657	25.234	6.8891
DMF	6.08	390	25,641	2.34705	0.823234	11.1563	3.3737
DMSO	5.98	394	25,380	2.28939	1.66186	22.4208	6.5676

Table 3 DFT calculated linear first order hyperpolarizability (β_o) for **6a-6c** ($X10^{-30}$ esu)

β_o	6a	6b	6c
Toluene	82.04426518	82.04426518	102.7707489
Dioxane	80.55682137	79.68670073	99.71068233
DCM	116.4425202	113.5312623	144.3146756
$CHCl_3$	103.4826739	101.3554092	128.2542364
EA	109.0156252	106.5610698	135.1084113
Acetone	126.0520412	122.5130164	156.1124712
ACN	129.5023522	125.7238153	160.2953904
DMF	129.6977813	125.9056029	160.5334077
DMSO	130.6411062	126.7823651	161.6748385

[48–52]. The quasi-two-level model in place of the three level model using the density matrix formalism to a simpler Eq. 8 [53, 54].

$$< \gamma > \alpha \frac{1}{E_{eg}^3} \mu_{eg}^2 \left(\Delta\mu^2 - \Delta\mu_{eg}^2 \right) \quad (8)$$

The value $\frac{1}{E_{eg}^3} \mu_{eg}^2 \left(\Delta\mu^2 - \Delta\mu_{eg}^2 \right)$ appearing in the Eq. 8 may be termed as third order "solvatochromic descriptor". The values for quinoxaline **6a-6c** in various solvents are given in (Table 2, **S5**, **S6**). The values calculated are static dipole moment (μ), the mean polarizability (α_0), the anisotropy of the polarizability (Δα) the mean first hyperpolarizability (β_o) and static second hyperpolarizability (γ), of the quinoxaline **6a-6c** molecule in different polarity of solvents.

Solvent Dependency of NLO Properties of Carbazole Based Quinoxaline (6a-6c) by DFT

The linear polarizability (α) value of quinoxaline derivatives **6a-6c** tabulated in (**Table S7**). The first hyperpolarizability value of compound **6a-6c** was ranging from 130 X 10^{-30} (**6a**), 126 X 10^{-30} (**6b**) and 161 X 10^{-30} (**6c**) esu (Table 3) in DMSO. These values are greater than urea (0.38 X 10^{-30}) by 343 (**6a**), 333 (**6b**) and 425 (**6c**) times. The value of asymmetric quinoxaline **6c** is larger than the other derivatives, which proved that quinoxaline with asymmetric geometry passes the higher polarizability values.

Second Order Hyperpolarizability (γ)

The quinoxaline derivatives show very high γ values, by DFT calculation. The carbazole based quinoxaline show 1226.40 X 10^{-35} esu. (**6a**), 1251.57 X 10^{-35} esu. (**6b**) and 1509.53 X 10^{-35} esu. (**6c**) γ values by computationally (**Table S8**).

Charge Transfer Characteristics of 6a-6c

An efficient charge transfer in a Donor–π–Acceptor chromophore is responsible for the manifestation of NLO properties. Degree of delocalization or fractional degree of localization of the excess charge (C^2_b) and donor–acceptor coupling matrix value (H_{DA}) was calculated by Eqs. 8 and 9 respectively [55].

$$C_b^2 = \frac{1}{2}\left(1 - \sqrt{\frac{\Delta\mu_{\geq}{}^2}{\Delta\mu_{\geq}{}^2 + 4\mu_{\geq}{}^2}}\right) \quad (9)$$

$$H_{DA} = \frac{\Delta E_{\geq} \Delta\mu_{\geq}}{\Delta\mu_{\geq}{}^D} = \frac{\Delta E_{\geq} \Delta\mu_{\geq}}{\sqrt{\Delta\mu_{\geq}{}^2 + 4\mu_{\geq}{}^2}} \quad (10)$$

where,

$\Delta E_{\geq}$	vertical excitation energy
$\Delta\mu_{\geq}$	difference between the adiabatic dipole moments of the ground and excited states
$\Delta\mu^D_{\geq}$	difference in adiabatic state dipole moments
$\mu_{\geq}$	transition dipole moment

Table 4 Degree of delocalization (C^2_b), donor–acceptor coupling value (H_{DA}) and donor–acceptor coupling distance (R_{DA}) for the dyes 6a–6c in various solvent

Solvents	6a			6b			6c		
	C^2_b	H_{DA} (cm^{-1})	R_{DA} (A°)	C^2_b	H_{DA} (cm^{-1})	R_{DA} (A°)	C^2_b	H_{DA} (cm^{-1})	R_{DA} (A°)
Toluene	0.327	12,057	4.73	0.348	12,120	3.21	0.361	11,944	3.48
Dioxane	0.133	8787	2.66	0.247	11,034	5.25	0.237	10,665	4.12
DCM	0.188	10,131	4.35	0.246	10,993	4.60	0.186	9708	2.39
$CHCl_3$	0.270	11,470	5.72	0.274	11,438	4.35	0.258	10,996	4.04
EtOAc	0.285	11,600	4.43	0.250	11,021	2.01	0.277	11,188	3.11
Acetone	0.120	8452	2.67	0.219	10,582	4.86	0.203	10,111	4.61
ACN	0.163	10,195	8.74	0.137	9485	5.70	0.109	8601	5.02
DMF	0.496	12,820	4.15	0.204	10,229	5.07	0.173	9400	4.36
DMSO	0.151	9077	5.01	0.179	9687	4.90	0.178	9449	5.08

Donor–acceptor coupling matrix distance (R_{DA}) was calculated by Eq. 11 [56]

$$R_{DA} = 2.06 \text{ x } 10^{-2} \frac{\sqrt{\nu_{max} \epsilon_{max} \Delta\nu_{12}}}{H_{DA}} \quad (11)$$

where,

ϵ_{max} molar extinction coefficient at maximum absorption

$\Delta\nu_{12}$ full width at half maximum (FWHM) of charge-transfer band

Higher calculated values of $\boldsymbol{C^2_b}$ and $\boldsymbol{H_{DA}}$ for 6a suggested higher coupling between donor and acceptor in polar solvents while reverse situation was observed in 6b and 6c (Table 4). On the other hand $\boldsymbol{R_{DA}}$ values increased from nonpolar to polar solvents indicated good charge separation in polar solvents for all the dyes.

Conclusion

3,6-di(substituted quinoxalin) carbazole fluorophores were designed and synthesized successfully. Photophysical properties study revealed positive solvatochromism with strong intramolecular charge transfer between the donor carbazole and acceptor quinoxaline through the π-conjugation. Computed vertical excitations using B3LYP/6-31G(d) basic set are in good correlation with the experimental values. Solvent polarity functions correlated well with the ICT phenomenon in these fluorophores. Nonlinear optical properties have been evaluated by solvatochromic method using two-level quantum mechanical model and are found to be in good correlation with density functional theory calculated values. Due to good charge transfer in these novel molecules can be applied to OLED or DSSC applications with suitable molecular structural modifications.

Acknowledgements Rahul Telore is grateful to UGC-CAS for providing fellowship under SAP. Amol Jadhav is thankful to UGC for fellowship.

References

1. Loudet A, Burgess K (2007) BODIPY dyes and their derivatives: syntheses and spectroscopic properties. Chem Rev 107:4891–4932. doi:10.1021/cr078381n
2. Zheng K, Lin W, Tan L et al (2014) A unique carbazole–coumarin fused two-photon platform: development of a robust two-photon fluorescent probe for imaging carbon monoxide in living tissues. Chem Sci 5:3439. doi:10.1039/C4SC00283K
3. Sekar N, Umape PG, Lanke SK (2014) Synthesis of novel Carbazole fused Coumarin derivatives and DFT approach to study their Photophysical properties. J Fluoresc 24: 1503–1518. doi:10.1007/s10895-014-1436-6
4. Singh P, Baheti A, Thomas KRJ (2011) Synthesis and optical properties of Acidochromic amine-substituted benzo[a]phenazines. J Org Chem 76:6134–6145. doi:10.1021/jo200857p
5. Zheng ML, Fujita K, Chen WQ et al (2011) Comparison of staining selectivity for subcellular structures by carbazole-based cyanine probes in nonlinear optical microscopy. Chembiochem 12:52–55. doi:10.1002/cbic.201000593
6. Joule JA (1984) Recent advances in the chemistry of 9H-carbazoles. Adv Heterocycl Chem. Elsevier, pp 83–198
7. Morin J-F, Leclerc M (2001) Syntheses of conjugated polymers derived from N-alkyl-2,7-carbazoles. Macromolecules 34:4680–4682. doi:10.1021/ma010152u
8. Yoon KR, Ko S-O, Lee SM, Lee H (2007) Synthesis and characterization of carbazole derived nonlinear optical dyes. Dyes Pigments 75:567–573. doi:10.1016/j.dyepig.2006.07.004
9. Tsai J-H, Chueh C-C, Lai M-H et al (2009) Synthesis of new Indolocarbazole-acceptor alternating conjugated copolymers and their applications to thin film transistors and photovoltaic cells. Macromolecules 42:1897–1905. doi:10.1021/ma802720n
10. Ning Z, Fu Y, Tian H (2010) Improvement of dye-sensitized solar cells: what we know and what we need to know. Energy Environ Sci 3:1170. doi:10.1039/c003841e
11. Brunner K, van Dijken A, Börner H et al (2004) Carbazole compounds as host materials for triplet emitters in organic light-emitting diodes: tuning the HOMO level without influencing the triplet energy in small molecules. J Am Chem Soc 126: 6035–6042. doi:10.1021/ja049883a
12. Zhang D, Martín V, García-Moreno I et al (2011) Development of excellent long-wavelength BODIPY laser dyes with a strategy that combines extending π-conjugation and tuning ICT effect. Phys Chem Chem Phys 13:13026. doi:10.1039/c1cp21038f
13. Zhao YS, Fu H, Peng A et al (2008) Low-dimensional nanomaterials based on small organic molecules: Preparation and optoelectronic properties. Adv Mater 20:2859–2876. doi:10.1002/adma.200800604
14. Law KY (1993) Organic photoconductive materials: recent trends and developments. Chem Rev 93:449–486. doi:10.1021/cr00017a020
15. Haidekker MA, Brady TP, Lichlyter D, Theodorakis EA (2006) A ratiometric fluorescent viscosity sensor. J Am Chem Soc 128:398–399. doi:10.1021/ja056370a
16. Li Z, Dong YQ, Lam JWY et al (2009) Functionalized Siloles: versatile synthesis, aggregation-induced emission, and sensory and device applications. Adv Funct Mater 19: 905–917. doi:10.1002/adfm.200801278
17. Jadhav AG, Shinde SS, Lanke SK, Sekar N (2017) Benzophenone based fluorophore for selective detection of Sn2+ ion: experimental and theoretical study. Spectrochim Acta Part A Mol Biomol Spectrosc 174:291–296. doi:10.1016/j.saa.2016.11.051
18. Jadhav AG, Kothavale S, Sekar N (2017) Red emitting triphenylamine based rhodamine analogous with enhanced Stokes shift and viscosity sensitive emission. Dyes Pigments 138: 56–67. doi:10.1016/j.dyepig.2016.11.021
19. Yang Z, Zhao N, Sun Y et al (2012) Highly selective red- and green-emitting two-photon fluorescent probes for cysteine detection and their bio-imaging in living cells. Chem Commun (Camb) 48:3442–3444. doi:10.1039/c2cc00093h
20. Devaraj NK, Hilderbrand S, Upadhyay R et al (2010) Bioorthogonal turn-on probes for imaging small molecules inside living cells. Angew Chem Int Ed 49:2869–2872. doi:10.1002/anie.200906120
21. Huang TH, Whang WT, Shen JY et al (2006) Dibenzothiophene/oxide and quinoxaline/pyrazine derivatives serving as electron-transport materials. Adv Funct Mater 16:1449–1456. doi:10.1002/adfm.200500823

22. Son H, Han W, Yoo D et al (2009) Fluorescence control on panchromatic spectra via C-alkylation on Arylated Quinoxalines. J Org Chem 74:3175–3178
23. Son HJ, Han WS, Wee KR et al (2008) Turning on fluorescent emission from C-alkylation on quinoxaline derivatives. Org Lett 10:5401–5404. doi:10.1021/ol802287k
24. Zhao ZH, Jin H, Zhang YX et al (2011) Synthesis and properties of dendritic emitters with a fluorinated starburst oxadiazole core and twisted carbazole dendrons. Macromolecules 44:1405–1413. doi:10.1021/ma1024957
25. Qi T, Liu Y, Qiu W et al (2008) Synthesis and properties of fluorene or carbazole-based and dicyanovinyl-capped n-type organic semiconductors. J Mater Chem 18:1131. doi:10.1039/b715920j
26. Zhang X, Shim JW, Tiwari SP et al (2011) Dithienopyrrole–quinoxaline/pyridopyrazine donor–acceptor polymers: synthesis and electrochemical, optical, charge-transport, and photovoltaic properties. J Mater Chem 21:4971. doi:10.1039/c0jm04290k
27. Paley MS, Harris JM, Looser H et al (1989) A solvatochromic method for determining second-order polarizabilities of organic molecules. J Org Chem 54:3774–3778. doi:10.1021/jo00277a007
28. Chen L, Cui Y, Mei X et al (2007) Synthesis and characterization of triphenylamino-substituted chromophores for nonlinear optical applications. Dyes Pigments 72:293–298. doi:10.1016/j.dyepig.2005.09.008
29. Wang Y, Frattarelli DL, Facchetti A et al (2008) Twisted π-electron system electrooptic chromophores. Structural and electronic consequences of relaxing twist-inducing nonbonded repulsions. J Phys Chem C 112:8005–8015. doi:10.1021/jp8003135
30. Momicchioli F, Ponterini G, Vanossi D (2008) First- and second-order polarizabilities of simple merocyanines. An experimental and theoretical reassessment of the two-level model J Phys Chem A 112:11861–11872. doi: 10.1021/jp8080854
31. Qian Y (2008) 3,6-Disubstituted carbazole chromophores containing thiazole and benzothiazole units: synthesis, characterization and first-order hyperpolarizabilities. Dyes Pigments 76:277–281. doi:10.1016/j.dyepig.2006.08.040
32. Huyskens FL, Huyskens PL, Persoons AP (1998) Solvent dependence of the first hyperpolarizability of p-nitroanilines: differences between nonspecific dipole-dipole interactions and solute-solvent H-bonds. J Chem Phys 108:8161–8171. doi:10.1063/1.476171
33. Frisch MJ, Trucks GW, Schlegel HB, et al. (2009) Gaussian 09, revision C.01. Gaussian 09, Revis. B.01, Gaussian, Inc., Wallingford CT
34. Thomas KRJ, Tyagi P (2010) Synthesis, spectra, and theoretical investigations of the Triarylamines based on 6 H - Indolo[2,3- b]quinoxaline. J Org Chem 75:8100–8111. doi:10.1021/jo1016663
35. Treutler O, Ahlrichs R (1995) Efficient molecular numerical integration schemes. J Chem Phys 102:346. doi:10.1063/1.469408
36. Becke AD (1993) A new mixing of Hartree–Fock and local density-functional theories. J Chem Phys 98:1372. doi:10.1063/1.464304
37. Lee C, Yang W, Parr RG (1988) Development of the Colle-Salvetti correlation-energy formula into a functional of the electron density. Phys Rev B 37:785–789. doi:10.1103/PhysRevB.37.785
38. Casida ME, Jamorski C, Casida KC, Salahub DR (1998) Molecular excitation energies to high-lying bound states from time-dependent density-functional response theory: characterization and correction of the time-dependent local density approximation ionization threshold. J Chem Phys 108:4439. doi:10.1063/1.475855
39. Cossi M, Barone V, Cammi R, Tomasi J (1996) Ab initio study of solvated molecules: a new implementation of the polarizable continuum model. Chem Phys Lett 255:327–335. doi:10.1016/0009-2614(96)00349-1
40. Tomasi J, Mennucci B, Cammi R (2005) Quantum mechanical continuum solvation models. Chem Rev 105:2999–3093. doi:10.1021/cr9904009
41. Patil VS, Padalkar VS, Sekar N (2014) 2-methyl-4-oxo-N-(4-oxo-2-phenyl substituted-1,3-thiazolidin-3-yl)-3,4- dihydroquinazoline-5-carboxamides - a new range of fluorescent whiteners: synthesis and photophysical characterization. J Fluoresc 24:1077–1086. doi:10.1007/s10895-014-1387-y
42. Williams ATR, Winfield SA, Miller JN (1983) Relative fluorescence quantum yields using a computer-controlled luminescence spectrometer. Analyst 108:1067. doi:10.1039/an9830801067
43. Telore RD, Satam MA, Sekar N (2015) Push-pull fluorophores with viscosity dependent and aggregation induced emissions insensitive to polarity. Dyes Pigments 122:359–367. doi:10.1016/j.dyepig.2015.07.017
44. Chen Y, Ling Y, Ding L et al (2016) Quinoxaline-based cross-conjugated luminophores: charge transfer, piezofluorochromic, and sensing properties. J Mater Chem C 4:8496–8505. doi:10.1039/C6TC02945K
45. Stock LM (1972) The origin of the inductive effect. J Chem Educ 49:400. doi:10.1021/ed049p400
46. Kerber RC (2006) If It's resonance, what is resonating? J Chem Educ 83:223. doi:10.1021/ed083p223
47. Carlotti B, Flamini R, Kikaš I et al (2012) Intramolecular charge transfer, solvatochromism and hyperpolarizability of compounds bearing ethenylene or ethynylene bridges. Chem Phys 407:9–19. doi:10.1016/j.chemphys.2012.08.006
48. Oudar JL (1977) Optical nonlinearities of conjugated molecules. Stilbene derivatives and highly polar aromatic compounds. J Chem Phys 67:446. doi:10.1063/1.434888
49. Oudar JL, Zyss J (1982) Structural dependence of nonlinear-optical properties of methyl-(2,4-dinitrophenyl)-aminopropanoate crystals. Phys Rev A 26:2016–2027. doi:10.1103/PhysRevA.26.2016
50. Kwon OP, Jazbinsek M, Seo JI et al (2010) First hyperpolarizability orientation in asymmetric pyrrole-based polyene chromophores. Dyes Pigments 85:162–170. doi:10.1016/j.dyepig.2009.10.019
51. Mardar SR, Beratan DN, Cheng L-T (1991) Approaches for optimizing the first electronic hyperpolarizability of conjugated organic molecules. Science 80(252):103–106. doi:10.1126/science.252.5002.103
52. Cheng LT, Tam W, Stevenson SH et al (1991) Experimental investigations of organic molecular nonlinear optical polarizabilities. 1. Methods and results on benzene and stilbene derivatives. J Phys Chem 95:10631–10643. doi:10.1021/j100179a026
53. Dirk CW, Cheng L-T, Kuzyk MG (1992) A simplified three-level model describing the molecular third-order nonlinear optical susceptibility. Int J Quantum Chem 43:27–36. doi:10.1002/qua.560430106
54. Kuzyk MG, Dirk CW (1990) Effects of centrosymmetry on the nonresonant electronic third-order nonlinear optical susceptibility. Phys Rev A 41:5098–5109. doi:10.1103/PhysRevA.41.5098
55. Wang Q, Newton MD (2008) Structure, energetics, and electronic coupling in the (TCNE 2) - encounter complex in solution: a polarizable continuum study †. J Phys Chem B 112:568–576. doi:10.1021/jp0753528
56. Creutz C, Newton MD, Sutin N (1994) Metal—lingad and metal—metal coupling elements. J Photochem Photobiol A Chem 82:47–59. doi:10.1016/1010-6030(94)02013-2